Available online at www.sciencedirect.com
SCIENCE DIRECT
Sensors and Actuators B 107 (2005) 936–944
SENSORS AND ACTUATORS B CHEMICAL
www.elsevier.com/locate/snb

Magnetic field-assisted DNA hybridisation and simultaneous detection using micron-sized spin-valve sensors and magnetic nanoparticles

D.L. Graham[a,*], H.A. Ferreira[a,b], N. Feliciano[a], P.P. Freitas[a,b], L.A. Clarke[c], M.D. Amaral[c,d]

[a] *Institute of Engineering of Systems and Computers-Microsystems and Nanotechnologies, Rua Alves Redol 9, 1000 Lisbon, Portugal*
[b] *Instituto Superior Técnico, Department of Physics, Avenida Rovisco Pais, 1000 Lisbon, Portugal*
[c] *Department of Chemistry and Biochemistry, Faculty of Sciences, Campo Grande, University of Lisbon, Portugal*
[d] *Centre for Human Genetics, National Institute of Health, Avenida Padre Cruz, Lisbon, Portugal*

Received 14 October 2004; received in revised form 13 December 2004; accepted 16 December 2004
Available online 15 February 2005

Abstract

Specifically designed on-chip microfabricated current-carrying metallic lines were used to generate local magnetic field gradients to facilitate the rapid focusing and hybridisation of magnetically labelled target DNA with complementary sensor-surface-bound probe DNA. Magnetoresistive biochips featuring high sensitivity spin valve sensors (2 μm × 6 μm) integrated within aluminium current lines, tapered in diameter from 150 to 5 μm at each sensor location, were surface functionalized with probe DNA and interrogated with 250 nm magnetic nanoparticles functionalized with complementary or non-complementary target DNA. Currents of 20 mA were used to rapidly concentrate and manipulate the magnetic nanoparticles at sensor sites in minutes, overcoming the diffusion limited transport of target DNA that leads to long hybridisation times. On-chip target DNA concentrations between ∼10 and 200 pM resulted in magnetoresistive hybridisation signals of ∼1–2 mV at 8 mA sense current, equivalent to ∼50–100 sensor-bound nanoparticles. The noise level (∼20 μV) was at the level of a signal calculated for a single nanoparticle (18.8 μV). Each nanoparticle was functionalized with <500 DNA molecules with an estimated 70 DNA–DNA interactions per nanoparticle at the sensor surface. The detection range was ∼140–14,000 DNA molecules per sensor equivalent to ∼2–200 fmole/cm^2. No binding signals were observed for magnetically labelled non-complementary target DNA.

Keywords: Magnetoresistive biochip; DNA chip; Spin-valve; Magnetic nanoparticle

1. Introduction

In addition to high sensitivity, selectivity and low sample volume, new biosensor and biochip platform technologies should preferably offer additional beneficial features including low cost device components and reduced assay times. In particular, there is a great need for more affordable and faster diagnostic DNA chip systems. Magnetoresistive (MR) bio-detection methodologies [1–4], based on sensor resistance changes resulting from magnetically labelled biomolecules binding to complementary magnetic field sensor-bound biomolecules, have already shown the potential to provide low cost devices, but reduced assay times have been hampered by the relatively slow diffusion of the magnetic labels to the on-chip sensor site(s). The majority of the detection platforms based on different types of MR sensor have utilized micron-sized magnetic labels of the size range 1–3 μm in diameter [5–12], but one immediate disadvantage is the very large size of the label in comparison to the biomolecules attached to the surface as this may hinder some biological interactions. Magnetic nanoparticles are more attractive in terms of size, but result in smaller sensor signals per label, hence detection systems utilising magnetic nanoparticles [13,14] normally require the use of high label concentrations in order to avoid slow, low gradient increases

* Corresponding author. Tel.: +351 21 3100300; fax: +351 21 3145843.
E-mail address: dgraham@inesc-mn.pt (D.L. Graham).

0925-4005/$ – see front matter © 2005 Elsevier B.V. All rights reserved.
doi:10.1016/j.snb.2004.12.071

in signal due to the gradual movement of the nanoparticles to the sensor. Here we show how we have overcome this diffusion barrier through the use of on-chip generated magnetic field gradients. As proof of concept for the development of magnetic field-assisted magnetoresistive DNA chips, we have demonstrated the rapid focusing of 250 nm diameter magnetic nanoparticles functionalized with target DNA at chosen on-chip spin valve [15] sensor sites. As a model probe, a wild type DNA sequence was chosen which is associated with the common and complex genetic disease cystic fibrosis (CF) [16,17]. This was a 50-mer oligonucleotide corresponding to the anti-sense strand of the cystic fibrosis transmembrane regulator (CFTR) gene, spanning the region of exon 10 where the most frequent CF-associated mutation, F508del, occurs [18,19]. To test the integrity of the detection method the probe was immobilised on the chip surface and interrogated with magnetic nanoparticles functionalized with complementary and non-complementary target DNA sequences. Hybridisation of the complementary target to sensor surface-bound probe was detected in real-time within minutes of introducing the magnetically labelled target DNA. This method is both fast and can employ low target DNA concentrations as the magnetic field gradients generated on-chip enable the user to effectively concentrate the magnetically labeled target DNA in the vicinity of the sensor.

2. Methods

2.1. Chip design and fabrication

The magnetoresistive chips featuring tapered current line structures were initially designed to demonstrate the controlled placement of single magnetic microspheres on top of spin valve sensors in order to illustrate the sensitivity of this detection platform [6]. The spin valve metallic multi-layer was fabricated using an ion beam deposition system on a 3 in. silicon wafer passivated with 500 Å Al_2O_3. The multi-layer structure consisted of Ta 20/NiFe 30/CoFe 25/Cu 26/CoFe 25/MnIr 60/Ta 30/TiW(N) 150 Å. As deposited, the spin valve coupon test sample had a magnetoresistance ratio (MR ratio) of ∼7.5%. The sensors were defined by standard photolithographic techniques and ion milling. Aluminum leads, 1 μm thick, were used to lead the sensor contacts to wire-bonding pads at the edge of the chip (Fig. 1(a)). After processing, the average MR of the sensor element was 5.5 ± 0.5%, the drop being due to contact and lead resistance. The average sensor sensitivity was found to be ∼0.06%/Oe (∼0.4 mV/Oe). Each chip was designed with six spin valve sensors, each sensor having two associated aluminium current line structures (3000 Å thick) tapered in diameter from 150 to 5 μm at sections adjacent to the sensor (Fig. 1(a) and (b)). Both sensors and leads were passivated with a 2000 Å thick sputtered SiO_2 layer for protection against fluid-based corrosion during experimentation. The silicon wafer was cut into individual 8 mm × 8 mm chips using a dicing saw.

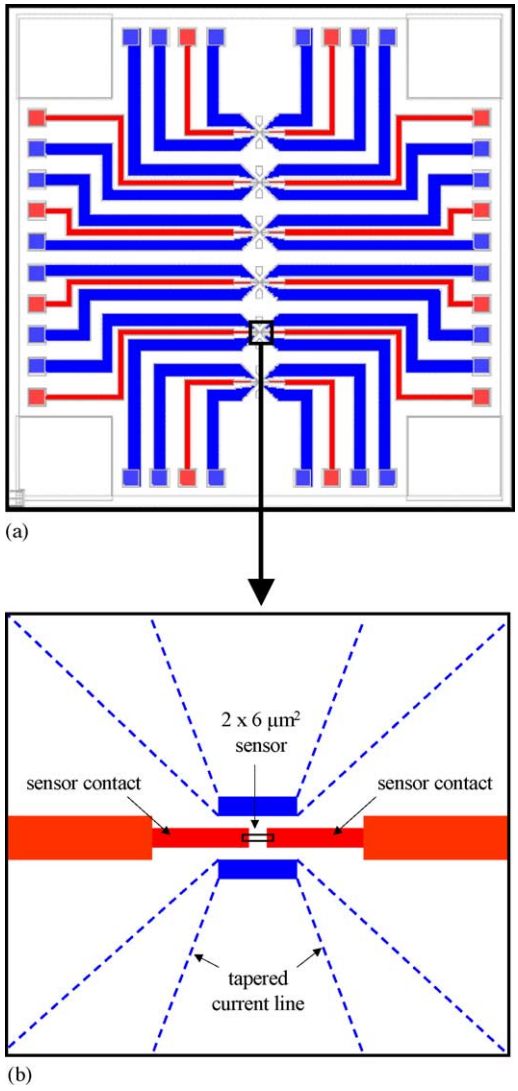

Fig. 1. (a) Schematic diagram of chip layout (dimensions 8 mm × 8 mm) featuring six single spin valve sensors (2 μm × 6 μm) fabricated in a line along the central region of the chip (sensor contact lines in red), each sensor having two associated tapered current line structures, one either side of the sensor line (current lines in blue). External contacts were made via the square contact pads around the edge of the chip. (b) A single spin valve sensor region showing the sensor lines (red) in relation to the tapered current lines (blue, dashed). For interpretation of the references to color in this figure legend, the reader is referred to the web version of the article.

Detection experiments were performed on chips mounted in 40-pin chip carriers. The contacts were made by wire bonding protected with an air-drying silicon gel (Elastosil E41, Wacker, Germany), which also created an on-chip well in which to perform all of the fluidic steps of biological experiments.

2.2. Magnetic nanoparticles

The superparamagnetic particles used were 250 nm diameter Nanomag®-D, composed of iron oxide (magnetite) dispersed in a dextran matrix (Micromod, Germany). The

magnetic moment per label was found to be $\sim 1.6 \times 10^{-13}$ emu for a 15 Oe magnetizing field [4].

2.3. The oligonucleotide-probe and target DNA sequences

A 50-mer oligonucleotide probe corresponding to the anti-sense strand of the CFTR gene, spanning the region of exon 10, where the most frequent CF mutation, F508del, occurs, was designed in-house and commercially synthesised (MWG, Germany). The sequence was 5′-ATT-CAT-CAT-AGG-AAA-CAC-CAA-AGA-TGA-TAT-TTT-CTT-TAA-TGG-TGC-CAG-GC-3′. The probe was prepared in two batches, both batches having a 3′ thiol functional group for cross-linking purposes and one batch having a 5′-fluorescein label, which was used to visually verify immobilisation of the probe by fluorescence microscopy. The complementary and non-complementary target DNA sequences used were double stranded polymerase chain reaction (PCR) products amplified from exon 10 of the CFTR cDNA [18] and exons 4 and 5 of the unrelated proto-oncogene Rac1 [19], respectively. The sequences were 5′-TTT-CCT-GGA-TTA-TGC-CTG-GCA-CCA-TTA-AAG-AAA-ATA-TCA-TCT-TTG-GTG-TTT-CCT-ATG-ATG-AAT-ATA-GAT-ACA-GAA-GCG-TCA-TCA-AAG-CAT-GCC-AAC-3′ (96 bp, complementary sequence underlined) and 5′-CCT-GCA-TCA-TTT-GAA-AAT-GTC-CGT-GCA-AAG-TGG-TAT-CCT-GAG-GTG-CGG-CAC-CAC-T GT-CCC-AAC-ACT-CCC-ATC-ATC-3′ (75 bp). Both targets were 3′ end biotinylated using a 3′-end biotinylation kit (Pierce, USA).

2.4. Immobilisation of CFTR probe

DNA probe immobilisation was first tested on SiO_2 samples (5 mm × 5 mm diced silicon wafer pieces with an RF-sputter-deposited layer of 2000 Å SiO_2) and SiO_2-passivated (8 mm × 8 mm) unmounted chips. The immobilisation protocol was optimised using fluorescence microscopy to qualitatively assess the density of immobilised fluorescently labelled probe (using an Olympus CK40 binocular microscope fitted with a C4040-Zoom digital camera, Olympus, Germany). This protocol was then transferred to the immobilisation of non-fluorescent probe on chips mounted on 40-pin chip carriers. The chip surface was activated using a 15% (w/v) aqueous solution of 2-aminopropyltriethoxysilane (APTS) and after 30 min the APTS was washed away with excess distilled water. The surface was then treated with a heterobifunctional cross-linking spacer (0.7 mg/ml sulfo-EMCS, Pierce, USA) in 100 mM borate buffer, pH 8.5, containing 150 mM NaCl. After 2 h, this solution was removed and the surface washed with the same borate buffer, followed by phosphate-buffered saline (PBS, 100 mM phosphate buffer, pH 7, containing 150 mM NaCl). The probe DNA was then applied to the chip surface as a 3 μM solution in PBS. After 3 h any unbound probe was washed away using 100 mM phosphate buffer, pH 7, containing 1 M NaCl. The chip surface was then washed in PBS again and pre-hybridised in a solution of 2.0% (w/v) bovine serum albumin (BSA) in PBS for 2 h. After the pre-hybridisation step, the chip surface was washed again with PBS.

2.5. Functionalisation of magnetic nanoparticles with target DNA

The biotinylated double stranded DNA target solutions were added to separate suspensions of streptavidin-functionalized magnetic labels in 100 mM phosphate buffer, pH 7 and mixed gently for 3 h at room temperature. The relative quantity of magnetic nanoparticles and DNA solution was calculated to give a ratio of 1:500 magnetic particles:DNA molecules, based on the calculated number of streptavidin molecules per nanoparticle (∼500). This solution was then centrifuged in a bench-top centrifuge to pellet (deposit) the particles and resuspended in 100 mM phosphate buffer, pH 7. This step was repeated a further two times to remove any unbound DNA molecules. In the final step, the pellet of magnetic nanoparticles was suspended in the hybridisation buffer (50 mM histidine). In order to produce magnetic nanoparticles functionalized with single stranded target DNA molecules, the magnetically labelled double stranded target DNA samples were denatured at 95 °C for 5 min and cooled on ice, immediately prior to use on-chip.

2.6. Magnetic field-assisted hybridisation and simultaneous detection

The mounted chips with surface-bound probe were inserted into the measurement set-up. This consisted of a small breadboard housed within an aluminium noise reduction box. Co-axial cables were used to make the electrical connections to power sources and a general-purpose interface bus (GPIB)-controlled multi-meter. A small (5 cm diameter) planar electromagnet with a $Ni_{80}Fe_{20}$ circular core was positioned over the chip carrier in order to apply an in-plane magnetic field (15 Oe). Images of magnetic label movements and binding to the chip surfaces were recorded using a Leica DMLM light microscope fitted with a JVC 3-CCD colour video camera (Leica Microsystems, Portugal). All of the hybridisation experiments were performed on-chip in 10–20 μl volumes of 50 mM histidine buffer. The detection experiments were performed by measuring the voltage drop across single sensors at 8 mA sense currents with a 15 Oe in-plane applied field. The experiments were performed as follows: the sensor was stabilised at 8 mA sense current to give a stable magnetoresistive signal baseline; an aliquot of 2–4 μl of the DNA target functionalized magnetic nanoparticles was added to the on-chip buffer, a current of 20 mA was passed through one or both of the current lines associated with the sensor in use until the narrow region of the line(s) became saturated with magnetic labels; the current through the line(s) was then switched off leading to the saturation of the sensor

surface with the magnetic labels and finally, the sensor/chip surface was washed: the unbound magnetically labelled DNA was washed away using 1× sodium saline citrate (SSC) containing 0.1% sodium dodecyl sulphate (SDS) followed by a further wash with 1× SSC. If a further cycle of these experimental steps was performed, the chip surface was first re-equilibrated in the hybridisation buffer (50 mM histidine).

2.7. On-chip temperature measurements

In order to estimate the temperature changes above the sensor surface, where temperature effects were the most crucial, a spin-valve sensor was calibrated for resistance (R) change with respect to temperature (T) by placing an unmounted chip on top of a hot plate and attaching a thermocouple to the chip surface. The resistance response of the sensor was measured at 1 mA sense current between 25 and 100 °C.

3. Results and discussion

3.1. On-chip magnetic field gradients

There are basically four on-chip magnetic fields to be considered: (i) the externally applied field; (ii) the attracting field produced by current passing through the tapered current lines; (iii) the smaller attracting field produced by the current passing through the sensor and (iv) the fringe field of the label. The applied field was constant across the chip surface, while the latter three fields were local. The magnetic nanoparticles act as both detectable labels (via their fringe field) and as biomolecular carriers [20] i.e. a means of transporting the target DNA molecules (via the attracting field produced by the current lines and to a lesser degree by the smaller attracting field of the sensor itself). The applied field is regulated through the current applied to an external electromagnet positioned over the chip. This is used both to induce an overall moment in the magnetic nanoparticles (i.e. align the small random moments of the iron oxide) to create a detectable fringe field and also to bias the sensor within the linear regime of its magnetoresistive (magnetic field) response curve [14]. The field produced by the current lines depends on the magnitude of the current and the current density. The current density is highest were the line dimensions are the smallest i.e., at the narrow regions of the tapered lines at either side of the sensor (shown as the solid blue regions in Fig. 1(b)). Consequently, when a current of sufficient magnitude (>10 mA) is passed through one or both lines a magnetic field energy profile is produced that favours the movement of the magnetic labels to the narrow regions of the line. The current through the sensor (1–8 mA) also produces an attracting magnetic field, albeit smaller than the field produced by the current line. Hence, when current flows through the lines, the magnetic labels are rapidly attracted to the narrow regions of the lines (by a force F_1) and when the current is switched off the particles are then attracted to the nearby sensor (by a force F_2) as represented schematically in Fig. 2. Thus either one or both lines can be used as a simple means to rapidly saturate the sensor surface with the nucleic acid-functionalized magnetic labels. Real images taken from a video recording made during an experiment in which one line was used to focus and detect 250 nm magnetic particles are shown in Fig. 3.

3.2. Hybridisation experiments with magnetically labelled target DNA

Hybridisation experiments were performed in cycles, each cycle consisting of four stages: (1) introducing the

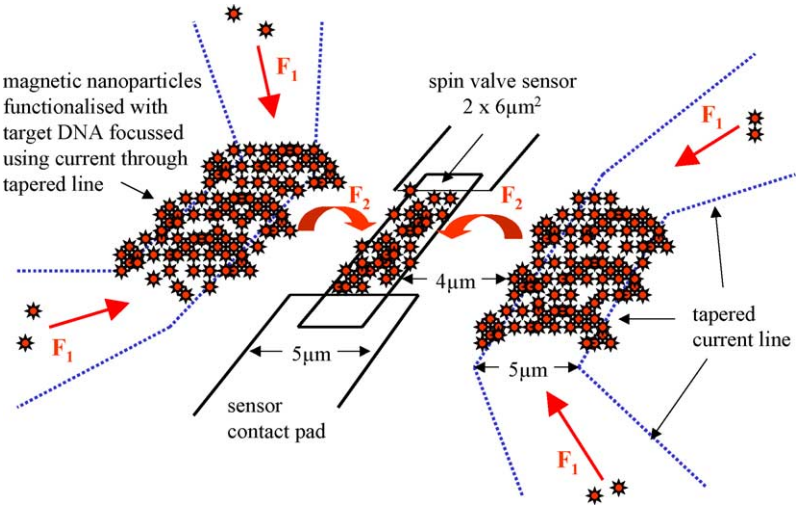

Fig. 2. A schematic representation of the operational principles of the tapered current line structures with a magnetoresistive spin-valve sensor. When 20 mA is passed through both current lines at either side of the sensor (central), a magnetic field gradient is generated resulting in a magnetic force F_1 that attracts the magnetic labels to the narrow regions of the current lines. When sufficient number of labels have been concentrated on the current lines, the current is switched off and the magnetic labels are then attracted to the nearby sensor by a magnetic force F_2 resulting from the smaller magnetic field generated by the current (8 mA) through the sensor. Thus high concentrations of magnetically labelled target DNA are rapidly brought into close contact with sensor-bound probe DNA.

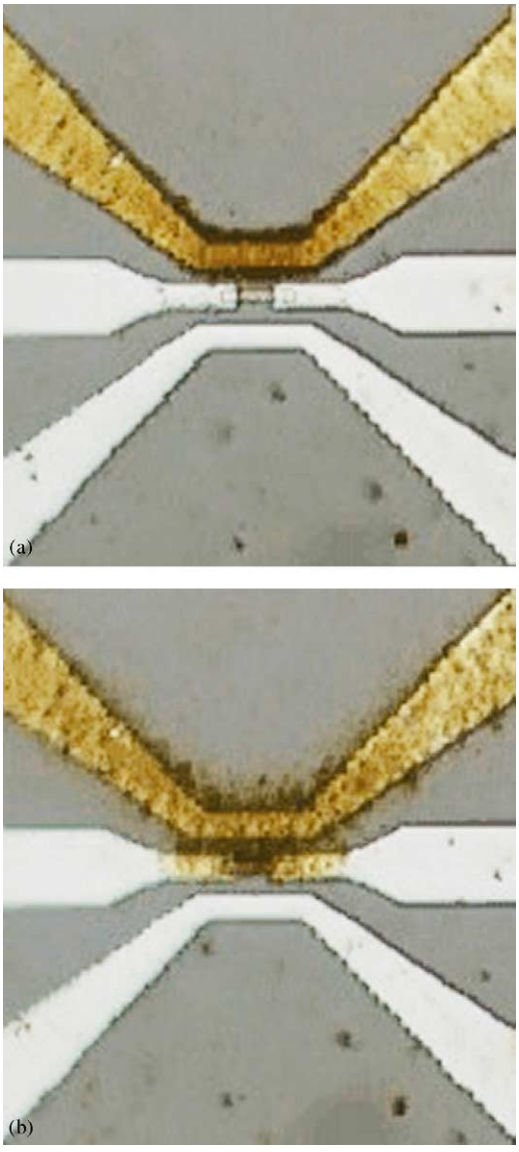

Fig. 3. Two still images taken from a video recording of the magnetic field-assisted focussing of 250 nm Nanomag®-D magnetic particles using one tapered current line at one side of a 2 μm × 6 μm spin valve sensor (sensor in the centre with central contact lines): (a) 20 mA current passed through the top tapered current line rapidly focuses the magnetic nanoparticles in the narrow region of the current line adjacent to the sensor. Note the increase in density of the nanoparticles on the line as the width decreases, resulting from increased current density. (b) Current through top line switched off and magnetic nanoparticles are attracted to and saturate the spin valve sensor.

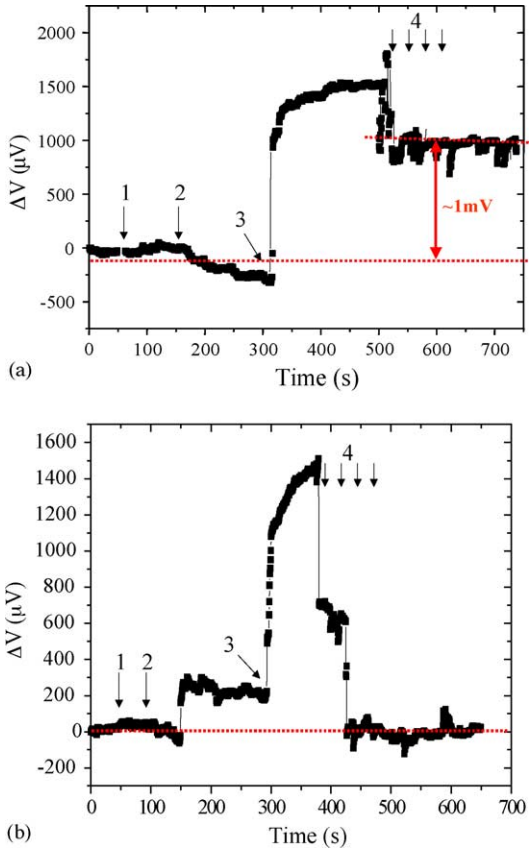

Fig. 4. Two magnetoresistive data charts showing the change in resistance of single 2 μm × 6 μm spin-valve sensors with time during magnetic field-assisted hybridisation experiments. A 50-mer CFTR wild type probe immobilised over the chip surface was hybridised with 250 nm Nanomag®-D particles functionalized with (a) complementary or (b) non-complementary target DNA at 8 mA sense current in an externally applied magnetic field of ∼15 Oe. The experimental cycle consists of: (1) addition of functionalized nanoparticles to the histidine buffer on-chip; (2) passing a current of 20 mA through both tapered current lines to attract the functionalized nanoparticles; (3) switching off the current through both current lines to effectively saturate the sensor with functionalized nanoparticles and (4) washing of the chip and sensor surface with buffer. A binding signal of ∼1 mV was observed with magnetic nanoparticles functionalized with complementary target DNA.

magnetic nanoparticles functionalized with single stranded target DNA; (2) passing a current through one or both of the tapered current lines to focus magnetic nanoparticles in high concentration at the narrow regions of the current line at each side of the sensor; (3) saturating the sensor by terminating the current through the current lines and finally (4) washing the sensor and chip surface. The duration of each cycle was ∼10 min with a sensor saturation time of ∼3 min. In the first experiments employing only one cycle, a current of 20 mA was passed through both tapered current lines to attract the magnetic labels and subsequently saturate the sensor (at 8 mA). After washing, a binding signal of ∼1 mV was obtained using magnetically labelled complementary target DNA (Fig. 4(a)). No binding signal was obtained for magnetically labelled non-complementary target DNA (Fig. 4(b)). However, this did not establish whether further hybridisation of the magnetically labelled complementary target DNA would occur on a more extended timescale. Consequently, experiments were performed employing two or three sequential cycles of sensor saturation and washing. The results obtained using only one tapered current line at 20 mA and the sensors at 8 mA are shown in Fig. 5. Once again only magnetically labelled complementary target DNA gave rise to binding signals. The first experimental cycle

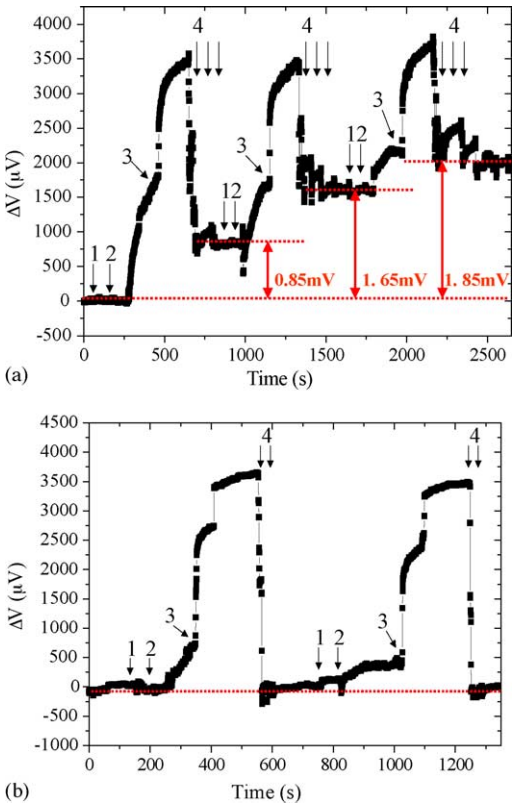

Fig. 5. Two magnetoresistive data charts showing the change in resistance of single 2 μm × 6 μm spin-valve sensors with time during magnetic field-assisted hybridisation experiments. A 50-mer CFTR wild type probe immobilised over the chip surface was hybridised with 250 nm Nanomag®-D particles functionalized with (a) complementary or (b) non-complementary target DNA at 8 mA sense current in an externally applied magnetic field of ∼15 Oe. The experimental cycle consists of: (1) addition of functionalized nanoparticles to the histidine buffer on-chip; (2) passing a current of 40 mA through both tapered current lines to attract the functionalized nanoparticles; (3) switching off the current through both current lines to effectively saturate the sensor with functionalized nanoparticles and (4) washing of the chip and sensor surface with buffer. Note with magnetic nanoparticles functionalized with complementary target DNA, a binding signal is obtained after each washing step. The hybridisation signal increases from 0.85 mV after one hybridisation cycle to 1.65 mV after two cycles and then to 2.0 mV after three cycles.

resulted in a binding signal of ∼0.85 mV, which increased to ∼1.65 mV after a second cycle and then to ∼2.0 mV after a third cycle (Fig. 5(a)). Calculations based on signal per label suggest that this binding signal represents ∼100 nanoparticles, representing >50% surface coverage of the sensor. It was calculated that a full monolayer of nanoparticles across the sensor surface (∼190 nanoparticles) would result in a signal of ∼3.6 mV at which point no further increases in the binding signal would be expected. In practice, 100% sensor coverage with nanoparticles would be difficult to attain due to steric hindrance at the binding surface. The absence of binding signals with magnetically labelled non-complementary target DNA indicated a negligible level of non-specific binding either with the probe DNA or with the sensor surface.

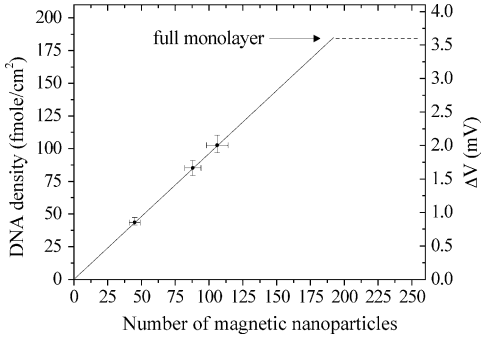

Fig. 6. A plot of the sensitivity and dynamic range of a single 2 μm × 6 μm with respect to the binding of 250 nm Nanomag®-D magnetic particles during magnetic field-assisted DNA hybridisation experiments. The conditions were 8 mA sense current, 15 Oe applied magnetic field and 20 mA current through one tapered current line associated with the sensor. The three points represent the binding signals obtained experimentally (see chart in Fig. 5(a)). The plot was based on calculations for the magnetoresistive signal that would be obtained for a single 250 nm magnetic label and calculations on the number of DNA molecules interacting at the sensor surface.

3.3. Sensor sensitivity and dynamic range

The determination of the number of target DNA molecules attached to each magnetic nanoparticle was based on the binding of one DNA molecule (via the 3′-end biotin) to each streptavidin molecule on the nanoparticle surface. The number of streptavidin molecules immobilised per nanoparticle was calculated using the total weight of streptavidin measured for a known bulk quantity of nanoparticles. The number of particle-bound target DNA molecules interacting with the probe DNA molecules above the sensor surface was then estimated by considering an 'arc' of the particle in contact with the sensor surface. This estimate was based on several assumptions: (i) the nanoparticle has a spherical shape; (ii) the streptavidin molecules are evenly distributed across the surface of the nanoparticle and (iii) the contact distance or height (h) between the sensor surface and the arc of the particle must not exceed the length of the probe DNA and cross-linker attached to the sensor surface (∼34 nm). When applied to Nanomag®-D particles with a diameter of 250 nm and radius (r) of 125 nm it was estimated that ∼500 streptavidin molecules were distributed across a surface area of $4\pi r^2 = 2.0 \times 10^5$ nm^2. Therefore, an arc of the particle $2\pi rh = 2.7 \times 10^4$ nm^2 in contact with the sensor surface represented ∼70 target DNA molecules interacting with sensor-bound probe DNA molecules [3]. The MR sensor signal resulting from a single magnetic nanoparticle bound to the sensor surface was estimated at 18.8 μV using the magnetic moment of the particle measured under the same experimental conditions employed during the detection process [4]. On this basis, the DNA detection range of a single 2 μm × 6 μm sensor was calculated at ∼140–14,000 molecules equivalent to ∼2–200 fmole/cm^2 (Fig. 6). The range of DNA concentrations that could be analysed on-chip vary considerably as this depends on the number of DNA molecules attached to each magnetic label. In principle, if one DNA molecule

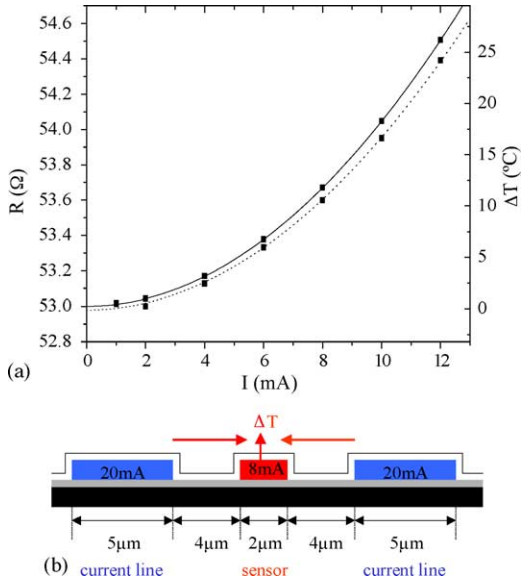

Fig. 7. (a) The temperature change above the spin valve sensor was determined via resistance measurements of the sensor at different sense currents (I) for positive currents (solid line) and negative currents (dashed line) using a calibration curve (not shown) for resistance versus temperature between 25 and 100 °C. (b) A cross-section through the chip in the region of a single sensor showing the distance of the sensor from the two associated current line structures. The temperature change (ΔT) calculated above the chip resulted from heating contributions from the current through the sensor itself and the current passing through one or both current lines.

was attached to each nanoparticle, then extremely low target DNA concentrations could be used. However, this approach would be unlikely to result in efficient hybridisation at the sensor surface, as the nanoparticles would have to be in the correct orientation to bind to the probe DNA. In practical terms, using reasonable number of target DNA molecules per label (10–50) it is anticipated that target DNA concentrations in the femto-molar range could be analysed on-chip.

3.4. On-chip temperatures at the sensor site

All of the on-chip hybridisation experiments were performed at room temperature. Nevertheless, the heat generated by on-chip structures during an experiment may be important as temperature changes may affect the sensor signal and may also affect biomolecular recognition processes such as hybridisation and dehybridisation. The temperature generated depends mainly on the magnitude of the currents used and the nature and the thickness of the insulating (or passivating) layers above and below the sensor or line structure. A calibration of sensor resistance versus temperature was performed and this was used to measure the sensor's thermal coefficient of resistivity: $1/R_0 \times \Delta R/\Delta T = 1.1 \times 10^{-3}\,^{\circ}\mathrm{C}^{-1}$, where R_0 is the room temperature resistance. This was then used to calculate the temperature change corresponding to an observed sensor resistance change at different positive or negative sense currents between 1 and 12 mA (Fig. 7(a)), illustrating a quadratic dependence ($\Delta T = K \times I^2$) on sense current (I). In order to avoid the magnetic effects of the different sense currents, the sensor was saturated in the parallel configuration by applying a magnetizing field of 50 Oe. The temperature change observed with an increase in current was almost instantaneous, with a negligible temperature increase observed over the following 10 min. At 8 mA (the sense current used in the DNA hybridisation detection experiments) the maximum temperature change was measured at ∼12 °C, resulting in a sensor surface temperature of ∼35–40 °C (without fluid based heat dissipation considerations): this temperature was close to the optimal temperature for the on-chip DNA–DNA hybridisation and well below the dissociation temperature of the CFTR target–probe DNA. The melting point calculated for the probe was 78.8 °C according to [21], although this does not take into account the DNA concentration and medium composition above the sensor surface. A similar temperature calculation using the sensor's resistance response was made for different currents passed through the two associated current lines at a 4 μm distance at each side of the sensor (Fig. 7(b)). The heat generated above the sensor as a result of a current of 20 mA passed through both associated current lines was found to increase the temperature at the sensor site by no more than 1–2 °C over 5–10 min operation.

4. Summary

We have demonstrated the first step in the successful development of magnetic field-assisted magnetoresistive-based DNA chips incorporating high sensitivity sensors and novel current line designs for rapid probe-target hybridisation using low target DNA concentrations. Other current line structures, such as micro-loops and matrixes, have previously been used to demonstrate the focussing or movement of magnetic beads or particles [22,23], but did not incorporate a functional detector for biomolecular recognition events. Our present goal is to demonstrate the detection of small structural differences in DNA or RNA sequences, such as wild type versus mutation sequences by careful manipulation of magnetically labelled target DNA. In addition, we aim to investigate other MR sensors (e.g. Planar Hall effect sensors [24]) and other on-chip current line structures in order to continue to improve the commercial potential of this new biochip platform.

Acknowledgements

This work was supported by the EU FP5 CF-Chip project, Contract No. QLK3-CT-2001-01982. H.A. Ferreira is grateful to the FCT, Portugal for doctoral grant (SFRH/BD/5031/2001) and the authors also thank the INESC-MN process engineers Fernando Silva and José

Bernardo for their help during chip processing and José Faustino for wire bonding.

References

[1] D.R. Baselt, G.U. Lee, M. Natesan, S.W. Metzger, P.E. Sheehan, R.J. Colton, A biosensor based on magnetoresistance technology, Biosens. Bioelectron. 13 (1998) 731–739.
[2] J.C. Rife, M.M. Miller, P.E. Sheehan, C.R. Tamanaha, M. Tondra, L.J. Whitman, Design and performance of GMR sensors in the detection of magnetic microbeads in biosensors, Sens. Actuators A: Phys. 107 (2003) 209–218.
[3] D.L. Graham, H.A. Ferreira, P.P. Freitas, Magnetoresistive-based biosensors and biochips, Trends Biotechnol. 22 (9) (2004) 455–462.
[4] P.P. Freitas, H.A. Ferreira, D.L. Graham, L.A. Clarke, M.D. Amaral, V. Martins, L. Fonseca, J.M.S. Cabral, Magnetoresistive DNA chips, in: M. Johnson (Ed.), Magnetoelectronics, Elsevier, Chapter 7, 2004, pp. 331–373.
[5] M.M. Miller, P.E. Sheehan, R.L. Edelstein, C.R. Tamanaha, L. Zhong, S. Bounnak, L.J. Whitman, R.J. Colton, A DNA array sensor utilizing magnetic microbeads and magnetoelectronic detection, J. Magn. Magn. Mater. 225 (2001) 138–144.
[6] D.L. Graham, H.A. Ferreira, J. Bernardo, P.P. Freitas, J.M.S. Cabral, Single magnetic microsphere placement and detection on-chip using current line designs with integrated spin valve sensors: biotechnological applications, J. Appl. Phys. 91 (10) (2002) 7786–7788.
[7] L. Lagae, R. Wirix-Speetjens, J. Das, D.L. Graham, H.A. Ferreira, P.P. Freitas, G. Borghs, J. De Boeck, On-chip manipulation and magnetization assessment of magnetic bead ensembles by integrated spin-valve sensors, J. Appl. Phys. 91 (10) (2002) 7445–7447.
[8] P.A. Besse, G. Boero, M. Demierre, V. Pott, R. Popovic, Detection of a single magnetic microbead using a miniaturized silicon Hall sensor, Appl. Phys. Lett. 80 (2002) 4199–4201.
[9] M.M. Miller, G.A. Prinz, S.F. Cheng, S. Bounnak, Detection of a micron-sized magnetic sphere using a ring-shaped anisotropic magnetoresistance-based sensor: a model for a magnetoresistance-based biosensor, Appl. Phys. Lett. 81 (2002) 2211–2213.
[10] G. Li, V. Joshi, R.L. White, S.X. Wang, J.T. Kemp, C. Webb, R.W. Davis, S. Sun, Detection of single micron-sized magnetic bead and magnetic nanoparticles using spin valve sensors for biological applications, J. Appl. Phys. 93 (10) (2003) 7557–7559.
[11] J. Schotter, P.B. Kamp, A. Becker, A. Pühler, G. Reiss, H. Brückl, A biochip based on magnetoresistive sensors, IEEE Trans. Mag. 38 (5) (2002) 3365–3367.
[12] J. Schotter, P.B. Kamp, A. Becker, A. Pühler, G. Reiss, H. Brückl, Comparison of a prototype magnetoresistive biosensor to standard fluorescent DNA detection, Biosens. Bioelectron. 19 (2004) 1149–1156.
[13] D.L. Graham, H.A. Ferreira, P.P. Freitas, J.M.S. Cabral, High sensitivity detection of molecular recognition using magnetically labelled biomolecules and magnetoresistive sensors, Biosens. Bioelectron. 18 (4) (2003) 483–488.
[14] H.A. Ferreira, D.L. Graham, P.P. Freitas, J.M.S. Cabral, Biodetection using magnetically labelled biomolecules and arrays of spin valve sensors, J. Appl. Phys. 93 (10) (2003) 7281–7286.
[15] P.P. Freitas, F. Silva, N.J. Oliveira, L.V. Melo, L. Costa, N. Almeida, Spin valve sensors, Sens. Actuators A: Phys. 81 (2000) 2–8.
[16] F.S. Collins, Cystic fibrosis: molecular biology and therapeutic implications, Science 256 (1992) 774–779.
[17] J.L. Bobadilla, M. Macek Jr., J.P. Fine, P.M. Farrell, Cystic fibrosis: a worldwide analysis of CFTR mutations: correlation with incidence data and application to screening, Hum. Mutat. 19 (2002) 575–606.
[18] A.S. Ramalho, S. Beck, M. Meyer, D. Penque, G.R. Cutting, M.D. Amaral, Five percent of normal CFTR mRNA ameliorates the severity of pulmonary disease in cystic fibrosis, Am. J. Resp. Mol. Biol. 27 (2002) 619–627.
[19] P. Jordan, R. Brazao, M.G. Boavida, C. Gespach, E. Chastre, Cloning of a novel human Rac1b splice variant with increased expression in colorectal tumors, Oncogene 18 (1999) 6835–6839.
[20] U. Häfeli, W. Schütt, J. Teller, M. Zborowski (Eds.), Scientific and Clinical Applications of Magnetic Carriers, Plenum Press, 1997.
[21] K.J. Breslauer, R. Frank, H. Blocker, L.A. Marky, Predicting DNA duplex stability from the base sequence, PNAS 83 (11) (1986) 3746–3750.
[22] C.S. Lee, H. Lee, R.M. Westervelt, Microelectromagnets for the control of magnetic nanoparticles, Appl. Phys. Lett. 79 (20) (2001) 3308–3310.
[23] T. Deng, G.M. Whitesides, M. Radhakrishman, G. Zabov, M. Prentiss, Manipulation of magnetic microbeads in suspension using micromagnetic systems fabricated with soft lithography, Appl. Phys. Lett. 78 (12) (2001) 1775–1777.
[24] L. Ejsing, M.F. Hansen, A.K. Menon, H.A. Ferreira, D.L. Graham, P.P. Freitas, Planar Hall effect sensor for magnetic micro- and nanobead detection, Appl. Phys. Lett. 84 (23) (2004) 4729–4731.

Biographies

D.L. Graham is a senior researcher at INESC-MN working on magnetoresistive biochip development. He graduated in applied biochemistry (1987) and completed his PhD in biotechnology (1992) at Liverpool JMU, UK. Since 1985 he has worked in a variety of biological and engineering research laboratories on multidisciplinary R&D projects in biotechnology, bioelectrochemistry and bioelectronics at the UK Atomic Energy Research Centre, Oxford University, Cranfield Institute of Technology, ICI/Zeneca, University College London in the UK and Instituto Superior Técnico (BERG) and INESC-MN in Lisbon. His present research interests include the use of magnetic and electric fields in bio-molecular studies, bioprocess optimization and bio-device development.

H.A. Ferreira is a graduate student in physics (2001) from Instituto Superior Técnico, Lisbon working on magnetoresistive biochip development. He is presently doing his PhD studies at INESC-MN.

N. Feliciano is a graduate student in physics (2003) from Instituto Superior Técnico, Lisbon. He was a senior project student at INESC-MN after graduation and is now involved in magnetoresistive biochip development.

P.P. Freitas received his PhD in solid-state physics from Carnegie Mellon University in 1986. His thesis topic involved the study of magnetoresistance in CoFe thin films. Between 1986 and 1987, he was a postdoctoral fellow at IBM, Yorktown Heights where he worked on magnetic thin films and high TC superconductors. Since 1990, he has been at the Instituto Superior Tecnico, where he is a professor in the Department of Physics. He is presently the director of INESC-MN and responsible for the magnetic recording technology research group. His current research interests include GMR heads for ultra high density recording, spin-dependent tunneling junctions, non-volatile memories, magnetic multilayers and thin films, micro-magnetism, transport phenomena, GMR sensors and bioelectronics.

L.A. Clarke graduated in zoology from the University of Bristol in 1990, and was awarded a PhD by the University of London in 1997 in the field of molecular endocrinology. He moved to the National Institute of Health in Lisbon in 1997 to undertake postdoctoral work on the role of alternative splicing in the expression of human mismatch repair genes. Since 2002 he has been involved in the characterization of cystic fibrosis-related patterns of gene expression using microarray technology at the University of Lisbon.

M.D. Amaral was awarded a PhD in molecular genetics in 1993 and is an associate professor in biochemistry working at the University of Lisbon and the Centre for Human Genetics, Lisbon on the molecular mechanisms that determine the pathophysiology of the genetic disease cystic fibrosis. Her research has been dedicated toward the understanding of the biogenesis, degradation and trafficking of the cystic fibrosis conductance regulator (CFTR) protein, product of the gene which, when mutated is responsible for CF. Her group has significant expertise in the molecular and cellular biology of CFTR, including proteomics approaches. Recent work involves the analysis of differential expression at the RNA level using a microarray approaches.